Carbon Fiber Components with Integrated Wiring for Millirobot Prototyping *

Ranjana Sahai
Mechanical Engineering Department
University of California, Berkeley
Berkeley, CA 94720 USA
rsahai@eecs.berkeley.edu

Erik Steltz and Ronald S. Fearing
Electrical Engineering and Computer Science Department
University of California, Berkeley
Berkeley, CA 94720 USA
ronf@eecs.berkeley.edu

Abstract **- We are developing a process to quickly prototype millirobotic systems in which the approach is to identify and develop a construction kit for fabricating almost any design, similar to the kits that are available for larger-scale robots. Two of the basic elements of the kit, the links and flexure joints, have been identified, and an assembly method has been developed. This paper deals with the problem of integrating the wiring in these parts, a significant task on this size scale. This novel feature is achieved through the use of a flexible ribbon cable consisting of three wires made out of patterned copper foil and polyimide. Low melting point solder has been tested successfully to make the electrical interconnect between the parts. We discuss the issues that must be addressed in designing the flexure-wiring combination. In addition, the paper presents the methodology for fabricating structures with integrated wiring using a simple four bar mechanism as an example. Finally, the tests show that the wiring loop over a flexure connecting a distally located sensor on the mechanism maintains both its electrical and mechanical integrity even during large motions. Future work will include the automated assembly of the parts with a low cost assembly tool.**

Index Terms – millimeter-scale robots, modular part construction, integrated wiring, flexure-based mechanisms.

I. Introduction

Miniaturization is a current trend in many areas of industry. Sectors such as information technology, aerospace, and medicine are all developing miniaturized robotic systems and measuring devices on the centimeter and sub-centimeter scale. Unfortunately, the design process is limited due to manufacturing processes that are often expensive and not easily accessible making the construction and testing of prototypes difficult.

This paper describes a process we are developing to quickly prototype various millirobot designs (millirobots are robots whose components are millimeter-sized). The approach being used here is to identify and develop key components that would then comprise a kit from which users could fabricate almost any design. This kit would be similar to robot kits that are readily available on the larger scale (like K'NEX®, LEGO® Mindstorms, etc.) and would include link elements, joints, actuators, and sensors. Wiring of distal actuators and sensors, which can be quite a challenge at this scale, would be incorporated into the parts and over joints in such a way that the assembly of the parts would also mean that most of the wiring is already complete. While the focus of the current work is on the development of basic kit parts and methods for integrating the wiring, future work will involve the automated assembly of the parts with a low cost assembly tool.

II. Background and Previous Work

Our group at University of California, Berkeley has done much work in developing methods for prototyping millirobotic structures ([1]-[5]). In the beginning, we prototyped the structures using folded stainless steel triangles (for the links) and polyester (for the joints). However, testing of these structures revealed significant peeling problems between the folded stainless steel triangles and polyester flexures. Hence, we decided to use carbon fiber instead of the folded stainless steel triangles for reasons described below.

The chief advantage this combination of carbon fiber and polyester has over the stainless steel/polyester one is ease of fabrication because it eliminates the need for folding and glue. The glue is unnecessary because the uncured carbon fiber epoxy matrix serves this role instead with the added advantage of eliminating the peeling problems mentioned earlier. Details of the use of this combination in building millirobotic structures can be found in [3].

Because of the size of the structures, building them by hand requires hours of tedious work under a microscope. For this reason, we have also done much work towards automating the building of these structures ([6]-[10]). Influenced by the work described above, we have moved towards fabricating more modular components using carbon fiber and polyester elements rather than cutting out entire specialized structures. This procedure is outlined in [10] and is described in more detail in the following section.

The study of rapid prototyping of mechatronic systems has lead to the development of some innovative manufacturing techniques such as some unique applications of 3D printing (for example, the shape deposition manufacturing techniques developed at Stanford [11]). Reference [12] describes the use of stereolithography techniques to create miniature versions of some classical type joints and small gears with embedded metal threads. The work presented here differs from [12] in the sense that rather than miniaturizing classical joints, we chose to take advantage of flexure joints, which are easily miniaturized and have no friction or backlash. Our focus is also directed toward developing a basic set of parts that a user can use to quickly prototype various designs without the use of highly specialized machines.

* This work has been supported by the following grants: NSF DMI-0423153, NSF DMI-0115091, and NSF IIS-0083472.

Several efforts towards integrating wiring as part of the assembly process have been reported in the literature. Most of this work (see [13] and [14], for example) involves embedding the wiring in the structure itself. Reference [15] suggests some innovative means of wiring including depositing wiring using soldering alloys and employing conducting polymers. A review of previous work in this area may be found in the above-mentioned papers. However, to our knowledge, millimeter-scale robotic parts with integrated flexure-wiring combinations capable of withstanding large-scale motion are unique to the present work.

III. Basic Carbon Fiber Components

Many basic robotic structures can be fabricated from simply two elements: links and revolute joints. For this reason, our first focus in developing our kit of parts begins with the fabrication and assembly procedure for these two basic elements. The first element simply consists of links of uncured carbon fiber. Several classes of widths and lengths of these uncured links will be provided. The second element is a flexure element that is constructed by sandwiching polyester in between carbon fiber, 1.5mm wide and 2mm long with a .125mm gap cut in the middle for the flexure length (again other gap lengths will be provided to allow variations in the desired flexure properties). Details of how these elements are fabricated are given in [10].

With these two elements, several types of structures can be fabricated as shown in Fig. 1. The general fabrication procedure calls for the user to assemble the links (either by hand or in an automated fashion) in their desired configuration on a slightly sticky surface (we use Gel-Pak®, see www.gelpak.com). Then the joint elements are placed on top. A thin sheet of Teflon is placed over the assembly and all of it is placed in a vacuum oven under weight and cured. After the assembly is cured, the structure is removed and folded into its final configuration. We tested this procedure by fabricating a four bar structure with a semi-automated procedure as described in [10].

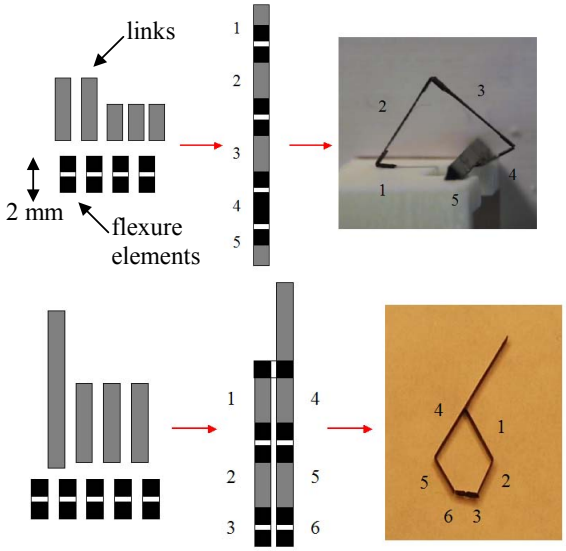

Fig. 1 Construction of four-bar and five-bar structures from links and flexure elements.

Unlike some of the larger-scale robotic construction kits, once the elements are assembled they cannot be easily disassembled and reassembled in a new configuration. However, in our experience during the design process, these prototype structures are likely to be subjected to destructive testing thus rendering the parts unsuitable for reuse anyway. Assembling the pieces in a 2D plane first and folding them into a 3D structure later has the advantage of lending itself to automated assembly (see [10]) and also to an integrated wiring scheme as described in the next section.

IV. Integrated Wiring

Several methods and materials for incorporating the wiring into the components were considered. For instance, since carbon fiber itself is conductive, we tested scenarios where the fiber was used as the wiring in addition to serving as a structural component. However, the use of copper foil (5µm thick) produced the most reliable electrical connections. We made the wiring by patterning the copper foil to create flexible and very thin "ribbon cables" that we could then incorporate into the links and over the flexure joints. The details of fabrication are given below:

(1) Copper foil is placed on Gel-Pak®, patterned (with a laser), and the excess is peeled off. The smallest cable made so far is 1.5mm wide with 150µm spacing between three wires.

(2) Adhesion promoter is applied to the patterned copper foil (either by spin coating or with a cotton swab).

(3) Polyimide (PI2525 or PI2611 from HD Microsystems, see www.hdmicrosystems.com) is spin coated on the patterned copper foil.

(4) The polyimide and copper foil are allowed to soft bake on a hot plate at approximately 100° C (higher temperatures may damage the Gel-Pak®) until the polyimide forms a film that is strong enough to be peeled off. This process takes 10 to 20 minutes.

(5) The ribbon cable is then hard baked on the hot plate for an additional 20 to 30 minutes at over 300° C to remove any remaining solvent. The finished product is shown in Fig. 2. The ribbon cable can now be cut into desired sizes and incorporated into the construction kit.

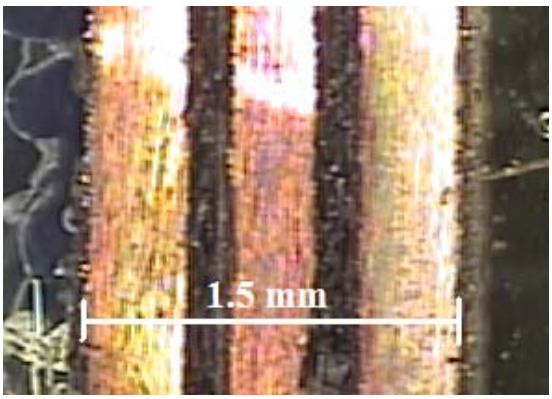

Fig. 2 Close-up of the finished ribbon cable.

Next, we considered the problem of making electrical interconnects between the individual components of the kit. Again several materials were considered. Anisotropic adhesives (substances that only conduct in the z-direction and not in the plane of the ribbon cable), both in the paste and film forms, were tried but were found to be very sensitive to the correct application of heat and pressure. Another alternative that was considered was the use of regular solder and solder paste, but the temperatures required to make the solder flow could potentially damage the structure and nearby sensors, etc. Finally, the substance chosen was a low melting point solder (TIX solder, it flows at 135° C). The details of its use are given below.

Before incorporating the ribbon cables (prepared as mentioned previously and cut to the desired sizes) onto the component pieces, their ends are tinned with the solder. This is accomplished by placing the pieces on the hot plate (at a temperature slightly higher than 135° C) with small pieces of low melting point solder situated on both ends. When the solder melts, it is smoothed by wiping a metal rod over it in the direction of the end of the piece. Although tests were done by trying to carefully apply anti-flux in the spacing between the copper wiring, it was found to be unnecessary since the solder naturally wets the copper surface but resists wetting the spacing in between the copper strips. It was also found that the solder could be applied in a "crayon fashion" by rubbing the ends of the ribbon cable pieces (while they are on the hot plate) with a stick of the low melting point solder. Fig. 3 shows a close up view of the results.

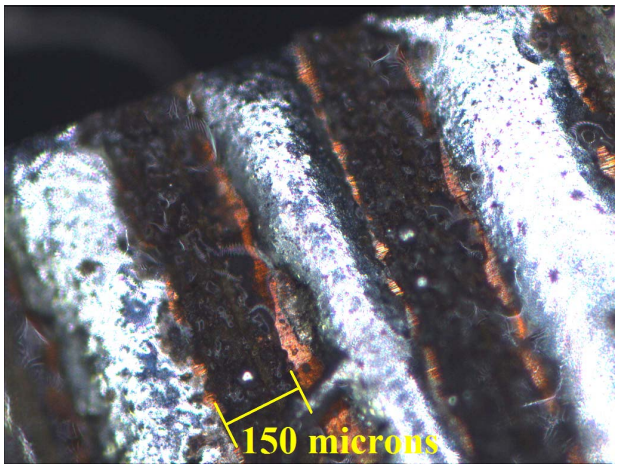

Fig. 3 Low melting point solder applied to the end of one of the finished ribbon cables.

Once the pieces have been tinned with solder, the ribbon cable that goes over the link elements are attached using uncured S-glass fiber in between the carbon fiber layer and the ribbon cable. The S-glass fiber is tacky when it is uncured and can serve as joining tape between the cable and link as well as an additional insulating element. The wiring over the flexure joints can then be accomplished as described in Fig. 4 where a loop of the ribbon cable is assembled over the joint. The length of the loop should be long enough so that the copper foil does not undergo much strain or interfere with the bending of the flexure.

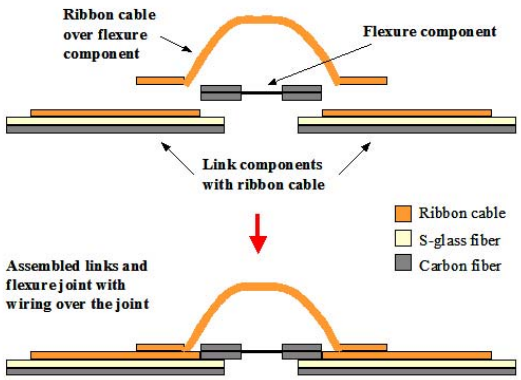

Fig. 4 Components and assembly method to accomplish the wiring over the flexure joints.

Initial tests on the connection between two pieces of the ribbon cable have been successful in the sense that they produce three continuous signals and virtually no crosstalk between the different wiring. Fig. 5 shows the results of one such test. Here two pieces of the ribbon cable that were tinned on both ends were assembled together on a piece of rubber. Heat at slightly over 135° C was applied by inverting the piece over a piece of glass on the hot plate for less than a minute. Testing each wire with a multimeter successfully validated their continuity. As described below, we have recently fabricated and tested a simple four bar mechanism with a strain gage and integrated wiring.

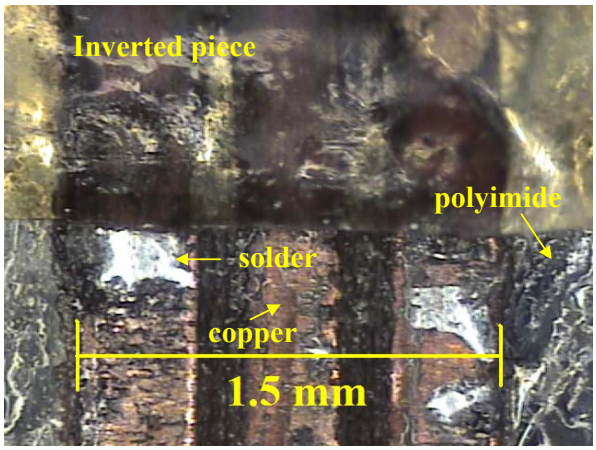

Fig. 5 Successful electrical interconnect between the two different pieces of the ribbon cable.

V. Fabrication of a Four-Bar Structure with Integrated Wiring

Although the above discussion was purposefully detailed, it should be noted that the actual construction of the parts would be done on a mass quantity size production scale so that the user simply has to take a kit of them and then just assemble the mechanism he or she wants to test. We tested this assembly method by fabricating a four-bar structure, meant to represent a leg of a crawling mechanism. We tested the integrated wiring by having a strain gage mounted on an extension of the output link of the four-bar

structure. Information gathered from the strain gage could then be used to detect contact of the leg with a surface.

The four-bar structure was fabricated in three parts consisting of the four-bar structure itself, a slider crank mechanism to attach it to the actuator, and the leg extension. We make the first two parts by placing a straight edge on the Gel-Pak® and assembling the links and then the flexure joints on top along this edge (similar to what is shown in Fig. 1). The slider crank is just a smaller version of the four-bar mechanism where two of the joints are fixed in a 90° configuration when it is assembled. The third part is just a link by itself that is glued on top of the output link as the leg extension. Two of the links are chosen with the integrated wiring on top of them, the last link after the output joint of the four-bar and the leg extension. The assembled parts are then covered with Teflon and put in the vacuum oven to cure with a weight placed on top of them. When cured, the parts are removed, and a strain gage is mounted on the extension. The slider crank and extension are then glued with super glue in their appropriate places and the wire ribbon is put in place from the leg extension to the last link after the output joint. It is sealed and the electrical connection made by simply rubbing a soldering iron (set to around 200° C) over the ends of the wire ribbon cable. The whole part is then mounted on a test stand (where the other end of the ribbon cable on the last link of the four-bar structure is used to mate with wires on the test stand) and is ready for testing (see Fig. 6).

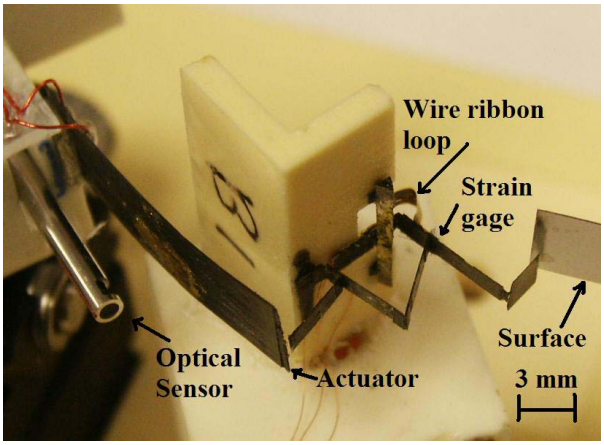

Fig. 6 Assembled four-bar leg mounted in place on the test stand. (Note: The actuator used here was not developed for this particular device. It is an oversized actuator used only for testing purposes.)

VI. Design Issues

Even though the four-bar structure presented above was built solely for demonstration purposes as a unique application of integrating wiring with flexure joints, we wanted to ensure that the mechanical integrity of the flexures would not be compromised during testing of the structure, and the wiring would not interfere with the functioning of the joints. Thus, we were motivated to perform the analysis below.

The stiffness of the flexure may be estimated from elementary beam theory as EI/d, where E is the Young's modulus, I is the cross-sectional moment of inertia, and d is the pivot length. The quantities that need to be specified to calculate the stiffness are the width (b), the thickness (h), and the length (d). It is noteworthy that the above relationship is accurate even when large deflections are involved if the flexure is subjected to only pure bending. The model is less accurate if transverse and axial loads are also present. For optimum performance, the flexure stiffness should be as small as possible. The stiffness can be reduced by decreasing E and I (since I is proportional to h^3, an effective way to reduce I is to reduce the flexure thickness) or by increasing the length d. The last option is not a desirable one since a long flexure may buckle easily.

For a simple (beam-type) flexure, the appropriate stiffness relations can be found in any strength of materials book and are given by equations (12-16) of Reference [16]. The quantities that should be considered when designing simple beam flexures include the axial stiffness (Ebh/d), the transverse or revolute stiffness ($Ebh^3/12d$), and the ratio of axial to transverse stiffness ($12/h^2$). Ideally, the last quantity should be as large as possible. The maximum rotation that a conventional flexure can go through before yielding is also an important parameter and is given by $\theta_{max} = 2d\sigma_y/Eh$. This last relationship can be easily derived from the formula for maximum bending stresses in a beam subjected to pure bending. Here σ_y represents the yield stress of the flexure material. As stated earlier, an important additional consideration in flexure design is the buckling of the flexure. Modeling the flexure as a link that is fixed at one end and free on the other, the critical strain, as determined from the standard column buckling relationships, is given by

$$\left(\frac{\sigma}{E}\right)_{crit} = \frac{\pi^2}{48}\left(\frac{h}{d}\right)^2 \qquad (1)$$

In order for the stress in the outermost fiber of the flexure not to exceed the yield strength of its material, the flexure length must exceed a critical value. This can be seen by considering the surface strain ε and stress σ in a beam bent elastically in a circular arc of radius R. These are given by

$$\varepsilon = \frac{h}{2R}, \quad \sigma = \frac{Eh}{2R} \qquad (2)$$

Hence the minimum value of R for σ not exceeding the yield strength is given by $Eh/2\sigma_y$. The minimum length for a given flexure is then given by $(R_{min})(\theta_{max})$.

It is clear from the above relationships that the material properties play an important part in flexure design. Ideally, the quantity σ_y/E should be as large as possible. The metals (σ_y/E = .004 for stainless steel) are therefore poor candidates for flexures. We choose polyester because of its relatively high σ_y/E value (.06) and superior adhesion properties. Based on the above calculations, we chose 12μm-thick polyester, 1.5mm wide and 125μm long.

Although the ribbon wiring cable forms a large loop, its mechanical parameters can be calculated by using straight beam flexure formulas presented above since the thickness of the ribbon is very small compared to the radius of the loop [17]. Since the ribbon cable wiring loops over and is parallel to the flexure, the total stiffness of the joint equals the sum of the stiffnesses of the ribbon and the flexure.

Calculations (using the above formulas with properties of copper) show that a ribbon cable exceeding a length of 1.5 mm will meet the minimum length requirements. Also, the wiring cable has stiffness an order-of-magnitude below that of the flexure. Hence our design meets our goal that the wiring should not restrain the motion of the device.

Although our intention at this stage is merely to demonstrate that our design of integrated wiring meets the fabrication requirements of the assembly goals described in the introduction, we are currently in the process of optimizing the design of a two degree of freedom, five bar leg with integrated wiring. The standard method of analyzing a flexure-jointed mechanism, at least for design purposes, is to use the so-called pseudo-rigid body model of the structure [18]. In this model, the compliant structure of the mechanism is replaced by a mechanism with rigid links and torsional springs (representing flexures) placed at the joints. It is then possible to analyze the mechanism by the standard and well-known procedures of rigid body kinematics and statics. More precise methods of analysis are currently under development in our lab (see [19]).

VII. Test Results

As mentioned in Section 4, we mounted the four-bar structure (built using the techniques described above) to a test stand along with an actuator, optical sensor, and a surface for the four-bar leg to hit in order to collect data on the structure. Our ultimate goal from these tests is to demonstrate that the kit and assembly methods produce viable structures for testing and prototyping millirobots. This includes integrated wiring that functions but does not interfere with the overall motion of the structure.

In the first tests, we drove the actuator with a low frequency (1 Hz) sine wave at various amplitudes (50, 70, 100, and 150V) for cases of the leg not tapping or tapping a surface. The purpose of these tests was to verify the motion of the structure and integrity of the wiring (which was done by collecting data from the distally wired strain gage). As an additional verification of the strain gage data collected, the displacement of the actuator was also tracked with an optical sensor (for more details on this sensor system, see [20]). The results are presented in Fig. 7 and 8. (It should be noted that the data for Fig. 7 and 8 were filtered with a 2^{nd} order lowpass Butterworth filter with a cutoff frequency of 500 Hz.) Fig. 7 shows the results from the optical sensor of the actuator movement for cases of the leg not touching the surface and two cases of it tapping the surface. As can be seen from these results, the optical sensor does show the differences in motion of the actuator when the leg contacts a surface but the points of actual contact with the surface and no contact with the surface are more easily derived from the strain gage data. This demonstrates the advantage of having a distally located sensor with the integrated wiring. The bottom graph in Fig. 8 shows the strain gages tracking the force at which the foot contacts the surface. There is an increase in force corresponding to increases in the amplitude of the actuator signal.

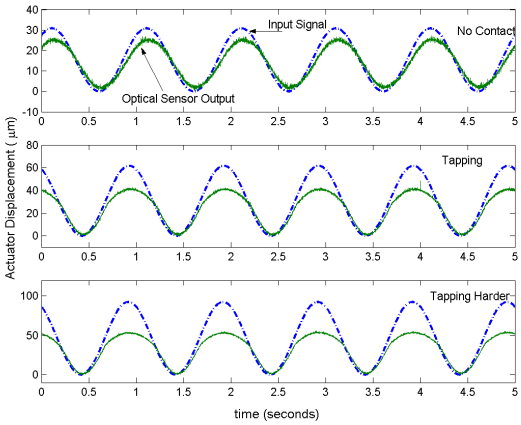

Fig. 7 Output from the optical sensors that are tracking the actuator displacement.

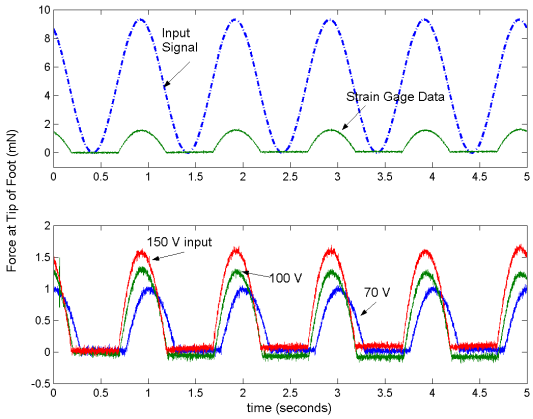

Fig. 8 Strain gage output of force at the foot tip.

The next set of tests performed was to show the integrity of the wiring (and hence the strain gage signal) as the structure goes through large angular displacements. To achieve this, the combination of the actuator and structure was run at resonance (around 180 Hz) while we recorded the optical sensor and strain gage data. During this test, the flexure at the output link was undergoing large angular motion of around 75° as can be seen from still shots of video taken at the low and high points of the motion (see Fig. 9). As can be seen from the pictures (and corresponded by the data), the wire loop around the flexure remains intact. Fig. 10 shows some of the data collected from the optical sensor and the strain gage. As demonstrated by the graphs, the actuator is undergoing around 300μm of motion and the strain gage is recording the forces due to the inertia of the foot. As expected, these signals are 180° out of phase.

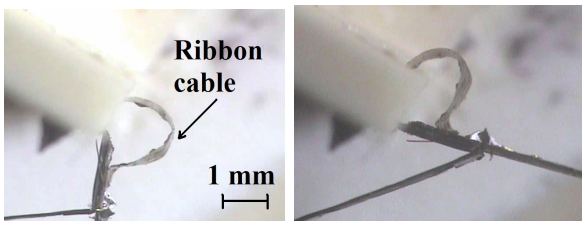

Fig. 9 Still shots from video taken of the output link as it undergoes large angular motion.

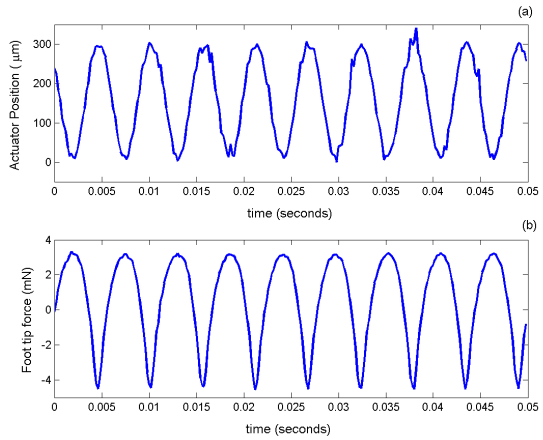

Fig. 10 (a) Optical sensor output of actuator displacement at resonance, and (b) force output from the strain gage due to inertia of the foot.

VIII. Summary and Future Work

We are developing a methodology for quick prototyping of millirobots that employs a construction kit of modular parts. It would allow the user to assemble the pieces of the kit in their desired design configuration to fabricate a variety of millirobotic systems. We have identified two basic components of this kit, the links and flexure joints made of carbon fiber, and developed an assembly method for them. The novel feature of this kit is the integrated wiring. A procedure for accomplishing this wiring through a flexible ribbon cable and low melting point solder has been developed and detailed. Tests of the electrical connection between pieces of the cable have also been successful. We have constructed a four bar mechanism with a distally located strain gage and recorded data while the mechanism is in operation. Through these tests, we have demonstrated the viability of structures fabricated by this method as prototypes and in particular the integrity of the integrated wiring around the joints as they go through large motions. In the future, we plan to further investigate the implementation of integrated wiring and develop a low cost tool for automating the assembly of the parts along with assembly algorithms for some common structures.

Acknowledgment

The authors would like to thank Srinath Avadhanula, Carmel Madjidi, and Robert J. Wood for useful discussions, and Richard Groff for useful discussions and assistance in providing a foot for the four-bar leg.

References

[1] Fearing, R.S., K.H. Chiang, M. Dickinson, D.L. Pick, M. Sitti, and J. Yan, "Wing Transmission for a Micromechanical Flying Insect," *IEEE Int. Conf. on Robotics and Automation*, April 2000, vol. 2, pp. 1509-1516.

[2] Moy, G., C. Wagner, and R.S. Fearing, "A Compliant Tactile Display for Teletaction," *IEEE Int. Conf. on Robotics and Automation*, April 2000, vol. 4, pp. 3409-3415.

[3] Wood, R.J., S. Avadhanula, M. Menon, and R.S. Fearing, "Microrobotics Using Composite Materials: The Micromechanical Flying Insect Thorax," *IEEE Int. Conf. on Robotics and Automation*, Sept. 2003, vol.2, pp. 1842-1849.

[4] Wu, W.C., L. Schenato, R.J. Wood, and R.S. Fearing, "Biomimetic Sensor Suite for Flight Control of a Micromechanical Flying Insect: Design and Experimental Results," *IEEE Int. Conf. on Robotics and* Automation, Sept. 2003, vol. 1, pp. 1146-1151.

[5] Yan, J., R.J. Wood, S. Avadhanula, M. Sitti, and R.S. Fearing, "Towards Flapping Wing Control for a Micromechanical Flying Insect," *IEEE Int. Conf. on Robotics and Automation 2001*, May 2001, pp. vol. 4, pp. 3901-3908.

[6] Shimada, E., et al., ``Prototyping Millirobots using Dexterous Microassembly and Folding," *Symp on Microrobotics, ASME Int Mech Eng Cong And Exp*, Nov. 2000, DSC-vol. 69-2, pp. 933-940.

[7] Thompson, J.A., and R.S. Fearing, ``Automating Microassembly with Ortho-tweezers and Force Sensing," *IEEE Int. Conf. on Intelligent Robots and Systems*, Oct. 2001, vol. 3, pp. 1327-1334.

[8] Sahai, R., J. Lee, R.S. Fearing, "Towards Automatic Assembly of Sub-Centimeter Millirobot Structures," *2003 NSF Design, Service and Manufacturing Grantees And Research Conference*, Birmingham, AL, Jan. 2003, pp. 1147-1156.

[9] Sahai, R., J. Lee, R.S. Fearing, "Semi-Automated Micro Assembly for Rapid Prototyping of a One DOF Surgical Wrist," *IEEE Int. Conf. on Intelligent Robots and Systems*, Oct. 2003, vol. 2, pp. 1882-1888.

[10] Sahai, R. and R.S. Fearing, "Improvements to a Semi-Automated Procedure for Rapid Prototyping of Millirobots with Applications," *2004 NSF Design, Service and Manufacturing Grantees And Research Conference*, Dallas, TX, Jan. 2004.

[11] Bailey, S.A., J.G. Cham, M.R. Cutkosky, and R.J. Full, "Biomimetic Robotic Mechanisms via Shape Deposition Manufacturing," *Robotics Research: The Ninth International Symposium*, J. Hollerbach and D. Koditschek, Eds. London: Springer-Verlag, 2000, pp. 403-410.

[12] De Laurentis, K., C. Mavroidis, and F.F. Kong, "Rapid Robot Reproduction," *IEEE Robotics and Automation Magazine*, June 2004, pp. 86-92.

[13] Cutkosky, M.R, et al. "Multimaterial, Multifunctional Systems via Shape Deposition Manufacturing," *NRO Final Report*, 2003, found at: www-cdr.stanford.edu/~motohat/publications/NRO_finalreport.pdf.

[14] Donald, B. R., et al. "Power Delivery and Locomotion of Untethered Microactuators," *Journal of Microelectromechanical Systems*, December 2003, vol. 12, no. 6, pp. 947-959.

[15] Malone, E. and H. Lipson, "Functional Freedom Fabrication for Physical Artificial Life," found at the following website: www.mae.cornell.edu/ccsl/papers/a**life**04_Malone.pdf.

[16] Goldfarb, M. and Speich, J. E., "A Well-Behaved Revolute Flexure Joint for Compliant Mechanism Design", *Journal of Mechanical Design*, September 1999, vol. 121, pp. 424-429.

[17] Hopkins, R. B., "Design Analysis of Shafts and Beams," *McGraw Hill.* 1970, p. 369.

[18] Howell, L. L., "Compliant Mechanisms," *John Wiley and Sons*, 2001, Chapter 5, pp. 135-218.

[19] Avadhanula, S. and R.S. Fearing, "Flexure Design Rules for Carbon Fiber Microrobotic Mechanisms," *IEEE Int. Conf. on Robotics and Automation 2005*, accepted.

[20] Steltz, E., S. Avadhanula, R.J. Wood, and R.S. Fearing, "Characterization of the Micromechanical Flying Insect by Optical Sensing," *IEEE Int. Conf. on Robotics and Automation 2005*, accepted.